Processing and Application of Ceramics 13 [3] (2019) 287–299
https://doi.org/10.2298/PAC1903287R

3D printing of kaolinite clay with small additions of lime, fly ash and talc ceramic powders

Carlos F. Revelo, Henry A. Colorado*

CC Composites Laboratory, Universidad de Antioquia UdeA, Calle 70 № 52-21, Medellín, Colombia

Received 22 February 2019; Received in revised form 19 June 2019; Accepted 15 August 2019

Abstract

Direct ink writing technique, an extrusion based additive manufacturing process, has been used to fabricate kaolinite clay based-ceramics with several inexpensive ceramic powders: lime, fly ash and talc. All the above materials are commonly used in the traditional ceramics industry, in both small and large industries, and therefore available worldwide. This research shows the simplicity of the process feasible not only for companies but also for individual users. The samples were fabricated with water to clay ratios (W/C) between 0.68 and 0.72. Additives were tested in 3.0, 5.0 and 7.0 wt.% with respect to the clay contents, although 3 wt.% of additives worked best. Cylindrical samples were fabricated with 20 mm in diameter and 20 mm in height in order to test their compressive strength and density. Measurement samples were previously cured for three days at room temperature and then exposed to 1100 °C for 1 h. The powdered additives and their corresponding mixtures with clay were characterized with scanning electron microscopy, X-ray fluorescence and X-ray diffraction techniques. Results showed that samples with 0.70 W/C ratio and using fly ash as an additive were the best in terms of workability, mechanical properties and surface finishing.

Keywords: *clays, 3D printing, traditional ceramics*

I. Introduction

Kaolinite clay is a naturally occurring commercial mineral available in many countries all over the world and it is one of the most commonly used materials in industry [1]. This material is typically used as an additive and a filler in paper coating formulations [2], ceramics [3], plastics [4], adhesives [4] and pharmaceutical [5] among others. Kaolinite is the essential component of kaolin consisting not only of basic aluminosilicates but also of a small amount of other phyllosilicates such as smectite, ilmenite, attapulgite and feldspar [6]. Typically, kaolin contains other minerals such as other phyllosilicates, feldspars, quartz, rutile, hematite, ilmenite, zircon, carbonates, sulphides and various kinds of ferrous and alumina hydroxides or oxo-hydroxides.

The rheological behaviour of kaolin clay suspensions is determined fundamentally by the properties of kaolinite particles [7]: particle size and distribution, morphology, aggregation, surface charge and chemical and mineralogical impurities. The differences in these properties control the behaviour of a kaolinite suspension against changes in pH, temperature and purity of water [8]. The final composition of kaolinitic raw materials depends on the geological process which took place during weathering of parent rocks (mainly granite, rhyolite, syenite, trachyte, gneiss and arcose) [9]. Thus, the development of this research was based on kaolinite clays from Colombia, the most abundant clays type in the region.

The world today demands new technologies for the production of ceramics that enable the industry to optimize the energy consumption and to minimize wastes by using them in other applications or processes. This is the case of using alternative ceramic materials like phosphates and geopolymers to hold large amount of wastes [10,11], traditional building materials with similar goals [12], or developing new manufacturing processes that use these unutilized materials [13]. Particularly in the processing, there is a limitation in the feasibility of traditional technology-related methods to produce complex-shaped ceramic-based parts with the desired compositions, microstructures and properties. Lastly, novel techniques have been developed, which include direct ink writing (DIW) also known as robo-

*Corresponding authors: tel: +57 321 4304877,
e-mail: *henry.colorado@udea.edu.co*

casting [14,15], solid freeform fabrication (SFF) [16], 3D printing (3DP) [17], selective laser sintering (SLS) [18], extrusion freeforming (EFF) [19], stereolithography (SLA) [20] and laminated object manufacturing (LOM) [21]. All these methods have become increasingly more important processing techniques in which three-dimensional objects are assembled by point, line or planar addition of materials, whose shapes are built by adding rather than subtracting [22]. Moreover, different innovations of the process such as printing in oil to control the water evaporation on extrusion process have been successfully proved [23].

In this work DIW technique was used [24] as a technique that offers a powerful option for the production of complex 3D structures using inexpensive materials and very simple and economically accessible process. In its simplest form, DIW can be used as a rapid prototyping tool for design that typically will be produced in large scale by traditional manufacturing. However, DIW also offers the potential to create 3D ceramic structures with locally varying geometry, composition, and properties which cannot be fabricated by the traditional ceramic technology [14]. Although ceramic additives in traditional ceramics industry are well-known to tailor process parameters and properties, in additive manufacturing there is a lack in the exploration of new and inexpensive materials. Additives for 3D printing processes [16,17] are quite important as they are very significant in both the final piece properties and the feasibility of the manufacturing process [13], economically and environmentally.

Research regarding the use of additives with DIW of clays and slurry base materials is of great importance not only for controlling its properties but also the rheology and other process parameters [25]. In clay and paste processing water is commonly used as dispersant to avoid the agglomeration and sedimentation of solid particles [26], and typically the use of deflocculants and dispersants is necessary in order to generate the appropriate flowing conditions for the fabrication [27]. These dynamic parameters can be tailored by optimizing the rheology of the mixture and the amount of solids in them [28].

In this work three types of additives were considered: lime (CaO), fly ash (C type) and talc ($H_2Mg_3(SiO_3)_4$). After the hydration process, the lime and talc most likely transformed to their hydrates form, $Ca(OH)_2$ and $Mg_3Si_4O_{10}(OH)_2$. These materials were selected not only based on their availability in Colombia but also worldwide. Their low cost and common use in the traditional ceramics industry were important factors as well. Other similar studies over different materials as additives have been successfully proved before including coal fly ash, lime, cement, and calcium chloride [29]. In the case of lime, fly ash and talc, many studies are reported showing their positive influence in clay-based materials by traditional manufacturing [29]. The present research aims to explain the role of lime, fly ash and talc in the DIW printing process of kaolinite clay. The main investigated parameters were: water ratio, sintering time and additive contents.

II. Experimental procedure

2.1. Sample preparation

Kaolinite clay powder was supplied from Sumicol S.A., Colombia, from La Paz mine. Its chemical composition is summarized in Table 1. Lime, fly ash and talc were acquired from local suppliers as well, all obtained from mines located in Colombia. All powders and clays were used as simple as possible, without beneficiation process, in order to prove the worst case scenario not only for small business enterprises but also for individuals like artists that use it as-extracted, typical in developing countries.

The manufacturing process used direct ink writing (DIW) 3D printing technique (Fig. 1), which was built from a modified apparatus originally used for printing plastics by the fuse deposition modelling technique (FDM). The extrusion printing device is an apparatus with a stainless steel frame, with Nema 17 Stepper motors, and four Stepper drivers DRV8825. Samples for compression and more complex parts were printed to evaluate their mechanical properties and show the limits of the process in terms of sample quality. The parts or printed structures were selected based on the main goals of the research: inexpensive material (no beneficiation process of the clay), inexpensive technique (local modified FDM machine), inexpensive process (no supporting material) and shapes that show potential for diverse products not only for industry but also for indi-

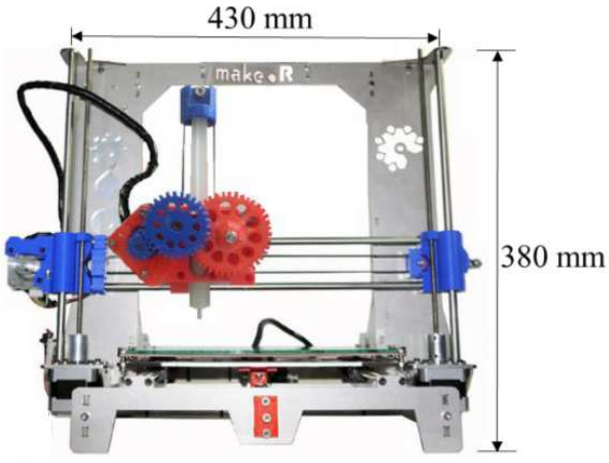

Figure 1. 3D printer used in this research

Table 1. Chemical composition (in wt.%) of the kaolinite clay from La Paz

SiO_2	Al_2O_3	Fe_2O_3	TiO_2	CaO	MgO	K_2O	BaO	MnO	P_2O_5	LOI at 1100 °C
61	23.2	2.39	2.65	0.09	0.17	0.29	0.01	0.03	0.02	10.2

Table 2. Fabricated formulations

	Samples with 3 wt.%			Samples with 5 wt.%			Samples with 7 wt.%		
W/C	0.68	0.7	0.72	0.68	0.7	0.72	0.68	0.7	0.72
Clay [wt.%]	58.48	57.8	57.14	57.80	57.14	56.50	57.14	56.50	55.87
Water [wt.%]	39.77	40.46	41.14	39.31	40.00	40.68	38.86	39.55	40.22
Additive [wt.%]	1.75	1.73	1.71	2.89	2.86	2.82	4.00	3.95	3.91
Total [wt.%]	100	100	100	100	100	100	100	100	100

viduals and artists. These conditions also help to build an education strategy in the topic which is mandatory now in developing countries for the innovation skill requirements that demand the new economic models: the Orange [30] and Circular Economy [31] models, even in the official goals of Colombia.

The samples were heated from room temperature to 1100 °C using ramp of 9.6 °C/min. After holding at 1100 °C/1 h oven was programmed to cool down which followed a similar ramp although this was not controlled. Cylindrical (20 mm diameter and 20 mm height) and more complex shapes were printed for characterization tests and for showing the feasibility of formulations for more complex and actual parts. Several sample combinations were made by mechanically mixing the clay powder with water and adding each of the following powdered materials: lime, fly ash and talc (Table 2). These additives were tested in concentrations of 3, 5 and 7 wt.% as recommended in previous research [32], although only sample with 3 wt.% were finally selected for the additive manufacturing based on the printing results. An overview of the samples is presented in Fig. 2 for W/C of 0.70. Based on previous results [13], three different water/clay ratios were investigated: 0.68, 0.70, and 0.72 W/C. It was found that W/C of 0.68 and 0.72 were not successful and therefore the investigation was conducted only over those able to be printed having W/C = 0.70.

For the printing process, all samples have been designed in the Repetier Host software. The cylindrical samples had 30 layers of clay distributed in filaments of 1.8 mm in diameter, all printed for 8 and 10 min. Dimension stability tests via thermal processing were conducted for the samples at three stages: immediately after finishing the printing process (green body or wet sample), after being cured for three days at room temperature (dry sample), and after the sintering process in a furnace at 1100 °C for 1 h (sintered sample). Five samples were tested for each of the successful formulations (W/C 0.68, 0.70 and 0.72), reporting in each stage its weight, height and diameter in order to determine percentages of shrinkage (between wet and dry samples) and ignition loss (between dry and sintered samples).

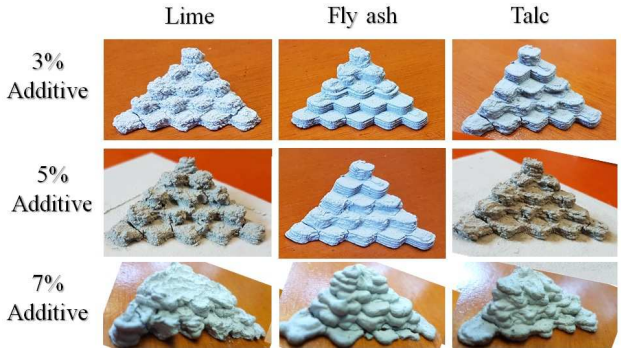

Figure 2. Overview of the samples with different compositions tested in this investigation for W/C 0.70

2.2. Characterization

Density tests were conducted for all samples with a Mettler Toledo balance according to the Archimedes' principle [33]. This method follows the standard procedure according to ASTM C373-14a, where dry weight (W_d), submerged weight (W_s) and saturated weight (W_{ss}) were measured, and the bulk density was estimated by $D_b = W_d/(W_{ss} - W_s)$.

Compression tests were performed in a Shimadzu AG250KN universal testing machine at 1.0 mm/min. Every successful formulation was tested over five samples and correspondingly reported.

X-ray diffraction (XRD) experiments were done in a PANalytical X'Pert PRO diffractometer (Cu Kα radiation of 1.5406 Å) at 45 kV with scanning between 10° and 90°. All XRD tests were conducted at room temperature. In order to determine the different phases present in the samples, Rietveld quantitative analysis was done using the software HighScore Plus from PANalytical B.V. Version 3.0.5. The global variables used for the analysis using the software were zero shift, mean deviation 0.005762, maximum 1.0, and minimum −1.0. In addition, the polynomial method was used in the global setting parameters. Finally, the crystal shape factor K was 1.0. X-ray fluorescence (XRF) tests of the clay were carried out in an ARL 8680 apparatus following the ASTM C114-03 procedure. Each powder additive (lime, fly ash and talc), including the pure clay powder without additives, was evaluated, in order to determine how each chemical element contributes to the ceramic sample.

Microstructure of the samples and raw materials were also investigated using scanning electron microscopy (SEM). For SEM the preparation of samples required a dehydration in a furnace at 30 °C for 24 h. The samples were also analysed with energy dispersive spectroscopy (EDS). All samples after the drying process were mounted on a carbon tape and gold sputtered with a Hummer 6.2 system, at conditions of 15 mA AC for 30 s, in order to make a thin film of pure gold. The SEM was a JEOL JSM 6700R in a high vacuum mode.

Particle size distribution was analysed by ImageJ software from SEM images, for which 100 measure-

ments of the particles diameters were taken. Thereafter, the particle distribution was analysed with the software Statgraphics by univariate analysis from normality of Shapiro Wilk, which is based on the quartile comparison of the normal distribution fit to data. As normal distribution did not fit the data well, other non-normal distributions were analysed, the gamma and log-normal distributions, by using the Kolmogorov-Smirnov proof as goodness-of-fit test. Finally, for qualitative analysis of the filament thickness and shape as a function of the additives, regular prismatic section was printed and analysed based on the global shape and the surface finishing.

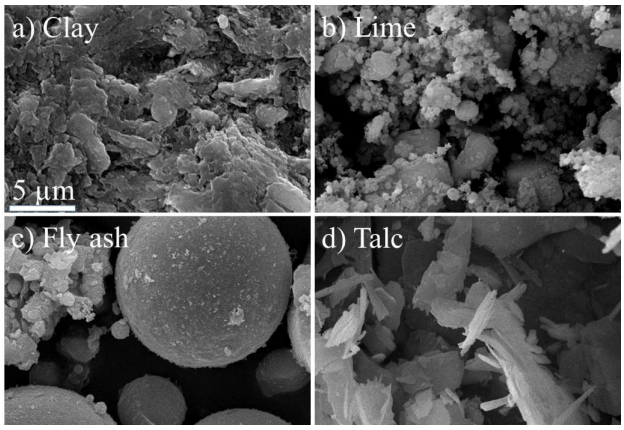

Figure 3. SEM images of raw additives: a) clay, b) lime, c) fly ash and d) talc

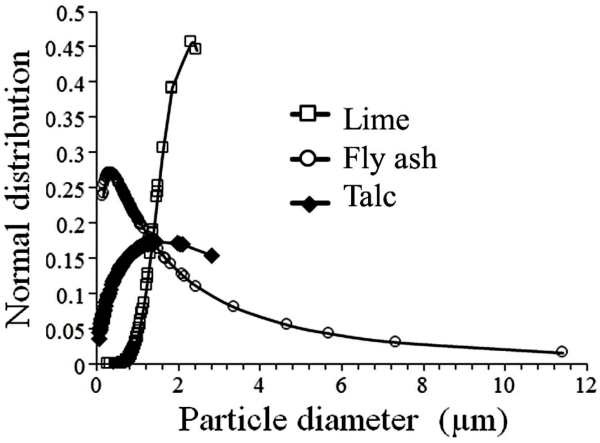

Figure 4. Particle size distribution of the raw powders additives

III. Results

SEM images of all raw solid materials (clay, lime, fly ash, and talc) are presented in Fig. 3. Clay powder from Fig. 3a reveals the typical layered structure, while Fig. 3b shows smaller and more amorphous particles for lime. Fly ash particles from Fig. 3c are shown as the typical mix of very symmetrical spherical and amorphous particles typical for this type of materials, and Fig. 3d shows a laminar structure of talc particles. The fly ash particles certainly have a shape more suitable to flow through the nozzle, when compared to other particle shapes of lime and talc. This opens up a new line of research regarding the optimal shape or combination of them to tailor the flow type of the 3D printing slurry.

Using multiple SEM images from the raw ceramic powders, particle size distribution curves were built for each particle type summarized in Fig. 4. From the mean particle size, talc gave the smallest particle size with 0.63 μm, followed by lime particles with 0.94 μm and fly ash with 1.08 μm. Figure 4 represents a non-normal distribution as a function of the particle diameter, where the log-normal distribution was developed for samples with lime and fly ash as additives, and the Gamma distribution was developed for talc as additive. From the statistical analysis, it is observed that both lime and fly ash have different skewness, due to the tails of the distribution which are lengthened to values below and above the mean, respectively, indicating a negative skewness for lime and positive skewness for fly ash. The results for the samples with talc as an additive show that the curve is almost symmetrical. The mean value of 1.08 μm for fly ash shows that their particles are dispersed and not concentrated in a single point. This means their distribution is not homogeneous, while the distribution range of lime and talc particles does not deviate to a great extent from the mean and median.

Elemental composition of the kaolinite clay, raw powder additives and their combination was determined by SEM-EDS. The corresponding elemental data are given in Table 3. SEM images for clay-additives powder mixtures, which reveal details of the effectiveness of the mixing process, are shown in Fig. 5. All images are taken just after the mixing process and before the sintering process. In all cases, the powders are well combined, without further agglomeration.

The dimensional changes after every stage of the production process are summarized in Fig. 6, carried out for

Table 3. SEM-EDS elemental characterization of the raw powder additives and their combination with kaolinite clay

Sample	C	O	Al	Si	Ti	Fe	Ca	K	Mg	Cl	V	total
Clay	29.22	32.56	13.47	21.17	1.07	1.99	-	0.37	-	0.14	-	100
Lime	5.66	43.52	-	0.25	-	-	50.19	-	0.39	-	-	100
Lime + clay	15.96	35.99	18.04	24.76	2.21	3.03	-	-	-	-	-	100
Fly	-	41.31	14.39	31.62	1.3	6.85	2.98	1.55	-	-	-	100
Fly + clay	10.16	42.55	18.02	21.84	2.07	3.28	1.74	0.33	-	-	-	100
Talk	-	40.83	4.44	27.94	-	8.19	2.66	-	15.94	-	-	100
Talk + clay	6.21	40.9	17.32	28.93	2.31	2.6	0.2	0.62	-	0.57	0.34	100

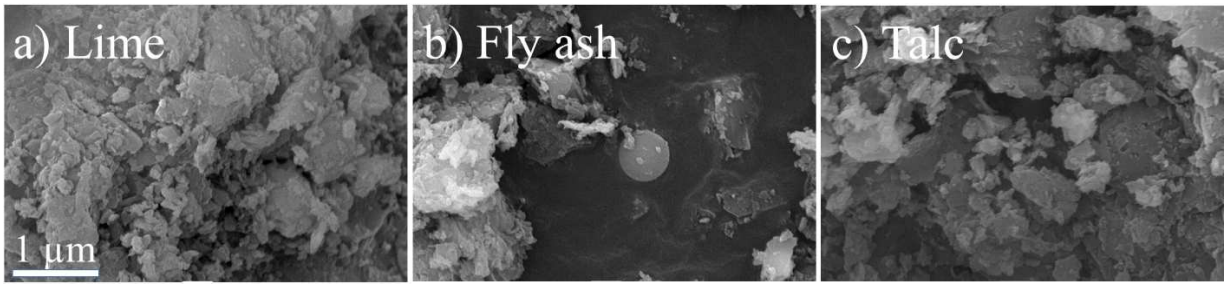

Figure 5. SEM images of clay-additives powder mixtures: a) lime, b) fly ash and c) talc

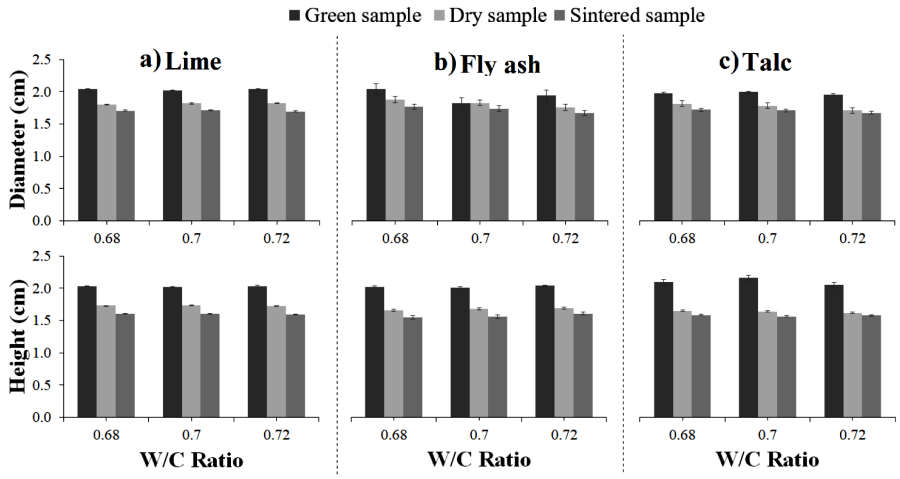

Figure 6. Dimensional changes (diameter and height) for samples made of clay with different additives: a) lime, b) fly ash and c) talc

the green body (wet sample), dried and sintered samples. It is clear that as the processing temperature increased, both diameter and height decreased. In general, there is no significant effect of the W/C over the sample contraction, although at higher concentrations of the additives probably distinct results could appear. This has not been explored in this research as the powder ceramics were used here as additives, in low concentrations.

Figure 7 was obtained from Fig. 6 and it summarizes the shrinkage of the diameter and height in Figs. 7a and 7b, respectively. Although there is diameter variation in the samples, this result is expected considering the material type used and the device utilized for the printing, which is summarized in the small error bars. The shrinkage over the diameter is about 10% less than the shrinkage over the height, which is associated mainly with the anisotropy in the sample introduced by the manufacturing technique (filaments were printed concentrically to the cylinder axis, and thus the release of water could be very different longitudinally than radially).

The percentages of weight loss during the drying and sintering are presented in Fig. 8. In general, the use of these additives generates higher weight losses during drying (wet-dry) than by ignition (dry-sintered) in all the W/C ratios. The effect of W/C on the weight loss is evident in Fig. 8a, confirming the expected result that more water in the mix increases the loss. Talc and lime showed a clear tendency to increase the weight loss with the water ratio, while fly ash just slightly increased. On the other hand, in Fig. 8b, lime and talc additions showed a very similar trend with a minimum point in 0.7 W/C. Fly ash addition kept the loos very constant

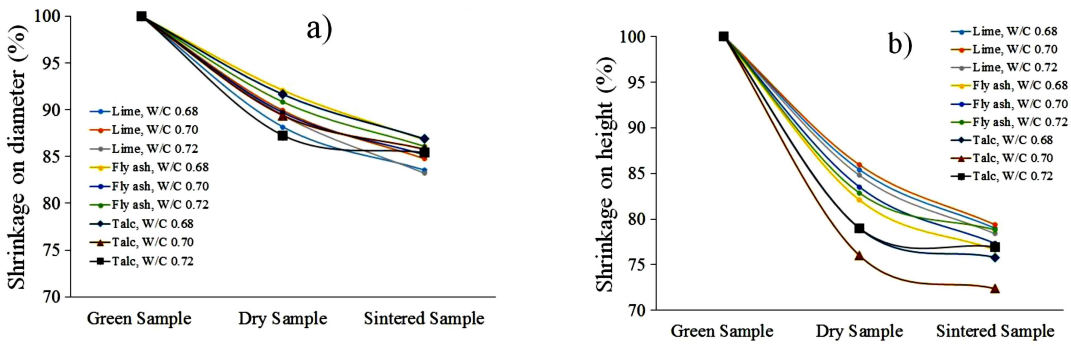

Figure 7. Shrinkage during thermal treatment in: a) diameter and b) height

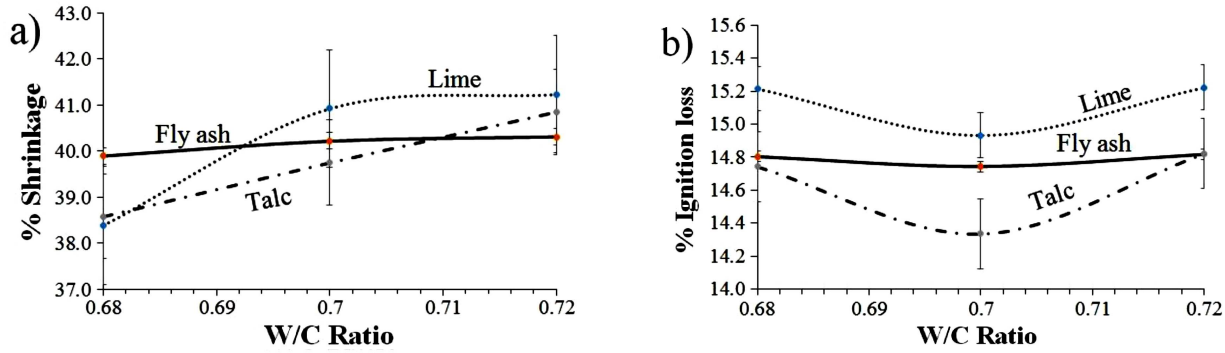

Figure 8. Percentage of weight loss: a) during drying and b) during sintering

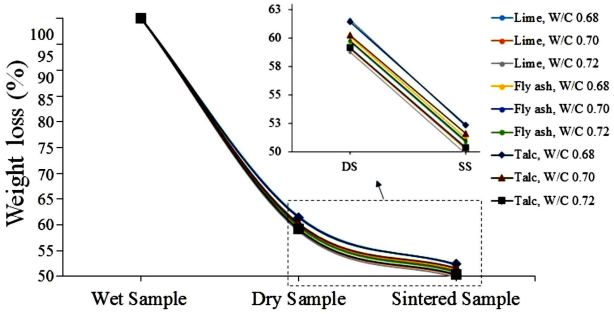

Figure 9. Weight loss results for all samples for three different additives and W/C ratios

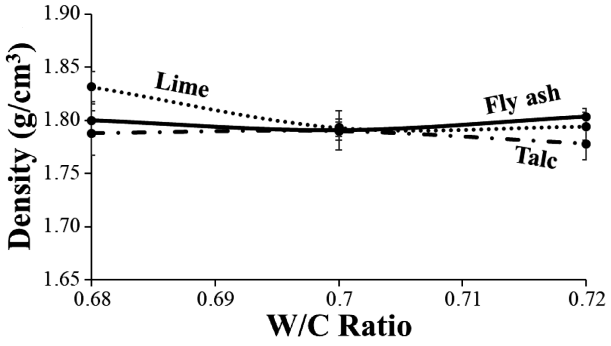

Figure 10. Density tests by the Archimedes balance method

with different W/C, and this suggests that the best formulation is with W/C 0.7. In addition, clays can show a higher porosity content after the firing process which could explain part of this significant weight loss [34].

Figure 9 shows the results of weight loss, where the weight of the wet samples was assumed as 100%. As expected, the weight loss from the wet to the dry samples was higher (about 40%) than the weight loss from the dry to the sintered sample (about 15%), which is explained by the amount of unbounded water released below 200 °C.

Densities, measured by the Archimedes method, are presented in Fig. 10. The results show that for W/C of 0.70 there is a minimum density value for the samples with fly ash and lime, while the samples with talc showed a weak maximum point. For W/C of 0.70 density was almost the same for the samples with different additives, however, for W/C of 0.68 and 0.72, these showed significant changes.

Compression strength results are presented in Fig. 11. The maximum compression strength for the sample free of additives is shown in Fig. 11a and it is similar to the value measured for W/C 0.7 in lime formulation. The samples with lime and talc show a maximum strength of 35 and 25 MPa, respectively. The samples with fly ash have compressive strength of about 20 MPa for W/C from 0.68 and 0.70, and for 0.72 W/C the compressive strength slightly increased to 23 MPa.

Figure 12 shows X-ray diffraction (XRD) data for the raw clay and for the three different formulations with additives after the sintering process. All phases were determined by the Rietveld quantitative analysis. Figure 12a for the raw clay revealed 69.8 wt.% kaolinite, 21.2 wt.% quartz, and 9.1 wt.% muscovite. In general, all samples composed from a mixture of the clay with the additive showing high quartz content. Figure 12b for

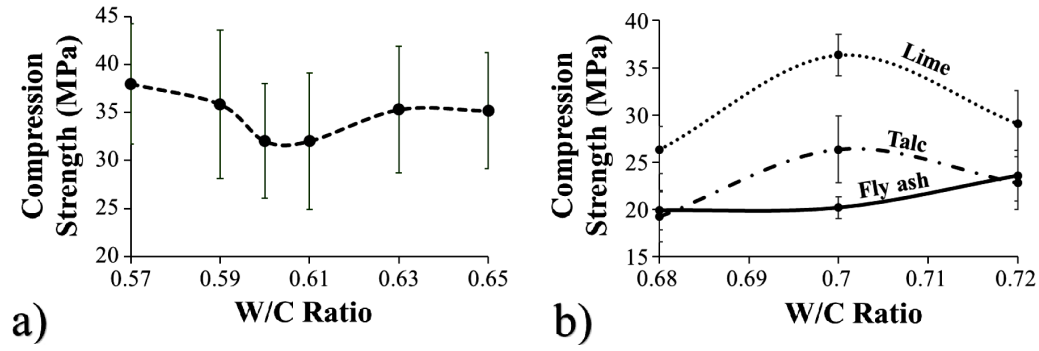

Figure 11. Mean of compressive strength results for: a) raw clay and b) clay with additives

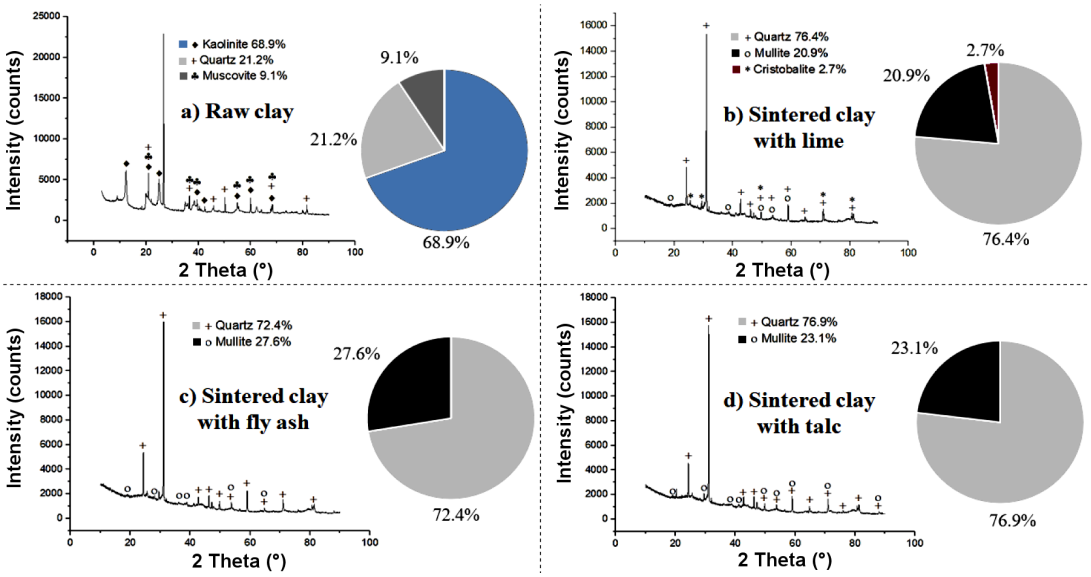

Figure 12. X-ray diffraction (XRD) of clay-additives mixtures: (a) raw clay, (b) sintered clay with lime, (c) sintered clay with fly ash, and (d) sintered clay with talc

clay with lime, shows 76.4 wt.% of quartz, 20.9 wt.% of mullite, and 2.7 wt.% of cristobalite. Figure 12c shows 72.4 wt.% of quartz, and 27.6 wt.% of mullite and Fig. 12d shows 76.9 wt.% of quartz, and 23.1 wt.% of mullite. Clearly, after the fabrication process is completed, the samples are mainly composed of quartz. Only sample of raw clay containing lime showed cristobalite. Quartz and mullite are also found in all the samples. It is observed that in all these sintered samples, the kaolinite phase did not appear because this phase suffers decomposition in other by-products due to the sintering process.

Figure 13 shows SEM images of the sintered clay with different additives fabricated using DIW technique. In general, all images revealed complex microstructures and also very irregular shapes. Unfortunately, the presence of the additives in the samples is not so clear in the images most probably because of their low concentration (3% of the amount of clay) and similar microstructure. Some micropores also appear in all samples, which

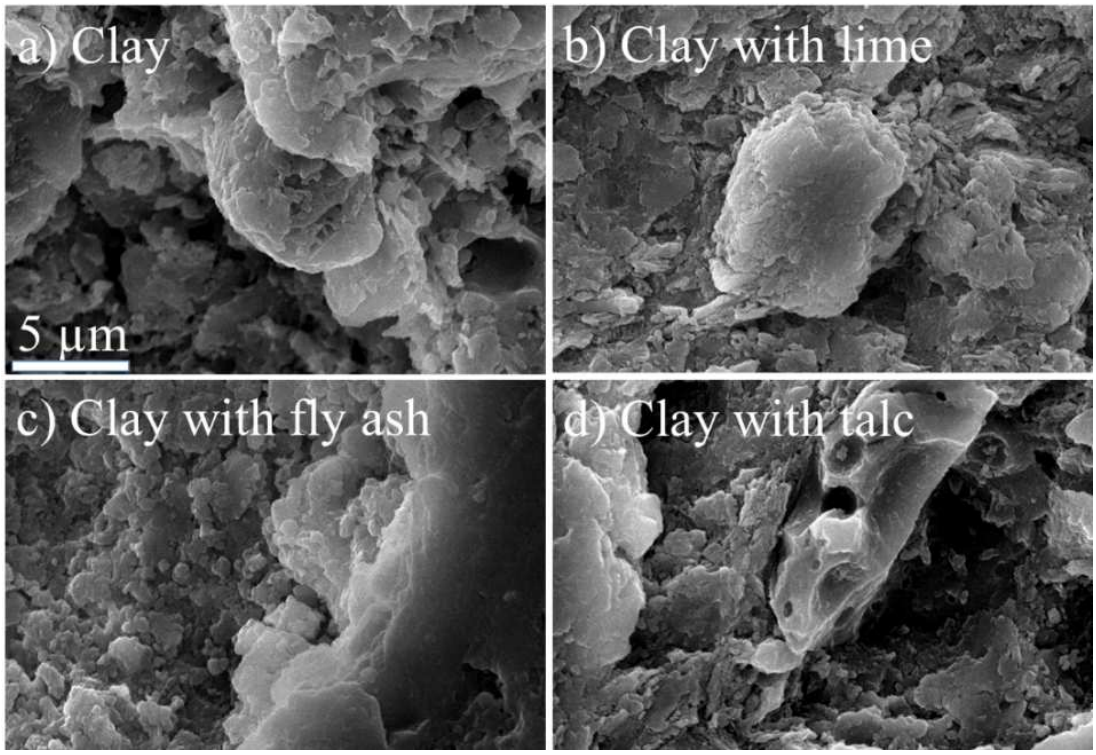

Figure 13. SEM images of the samples made by 3D printing after heat-treatment at 1100 °C: a) clay, b) clay with lime, c) clay with fly ash and d) clay with talc

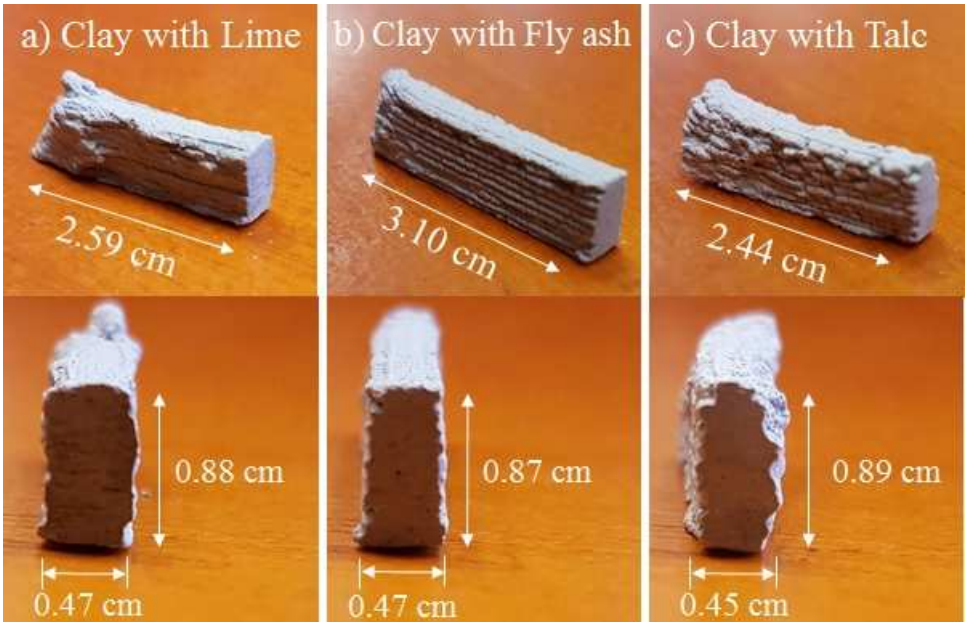

Figure 14. Filament thickness experiment for W/C 0.7 using different additives: a) lime, b) fly ash and c) talc

could be significant for the stability of the formulation because they contribute to the increase of pressure caused by the crystallization of soluble salts in the pore walls [35] and thus eventually produce micro-cracks that decrease the performance of engineering components. Nevertheless, fly ash particles could help to decrease pores in the sample as they can act as fillers [36].

Figure 14 shows 3D printing profiles of the clay with W/C 0.7 using lime, fly ash and talc. The sample with fly ash showed better conservation of the form and geometry in comparison with the structures of the other additives. Very well defined and constant filaments can be observed throughout the trajectory and a better stability of the piece. This has been associated with the shape and size of the particles, nearly perfectly spherical, which can flow more homogeneously through the nozzle and thus be better impregnated (less voids) than other particles used. Figure 15 shows details of the additive manufacturing process for a pyramid structure. It is obvious that the sample with fly ash is substantially better than those prepared using lime or talc as additives.

Figure 16 summarizes selected parts fabricated with the DIW apparatus and using the clay with fly ash addition. Figure 16a represents a "star bowl" container, which shows the basement of one single filament layer and the thick border with several filaments. Figure 16b is a clay vase showing a more complex structure for the simplicity of the material used (not optimized paste). Figure 16c shows a trapezoidal bowl, a container of one filament thick, which reveals the consistency of the clay stable in such a tilted structure; Fig. 16d is a top view of helical solid structure. These objects show that upon a manufacturing process optimization, any shape can be built and the finishing improved as well. It is important to note that no additional basements or support structures were needed for these parts.

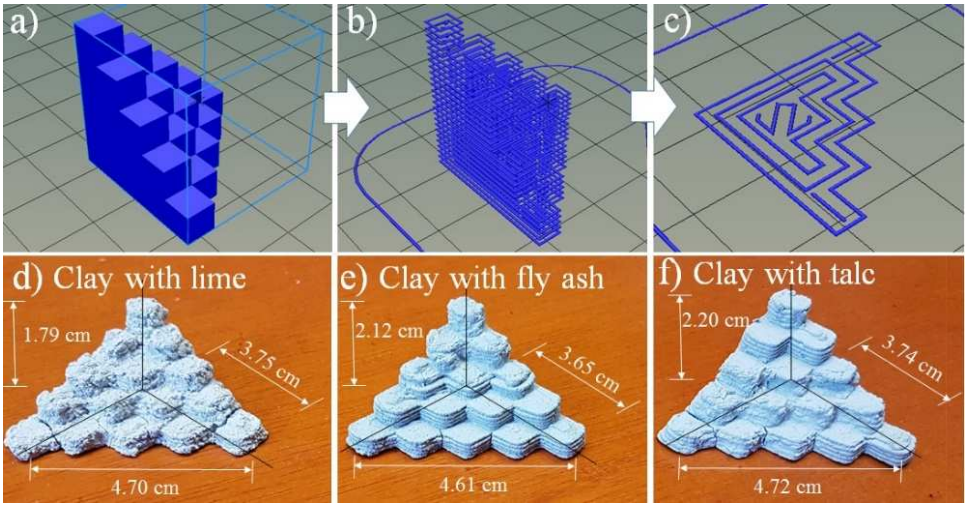

Figure 15. 3D printing process of a pyramid: a) solid design, b) layered design, c) first layer printing; printed parts using different additives: d) lime, e) fly ash and f) talc

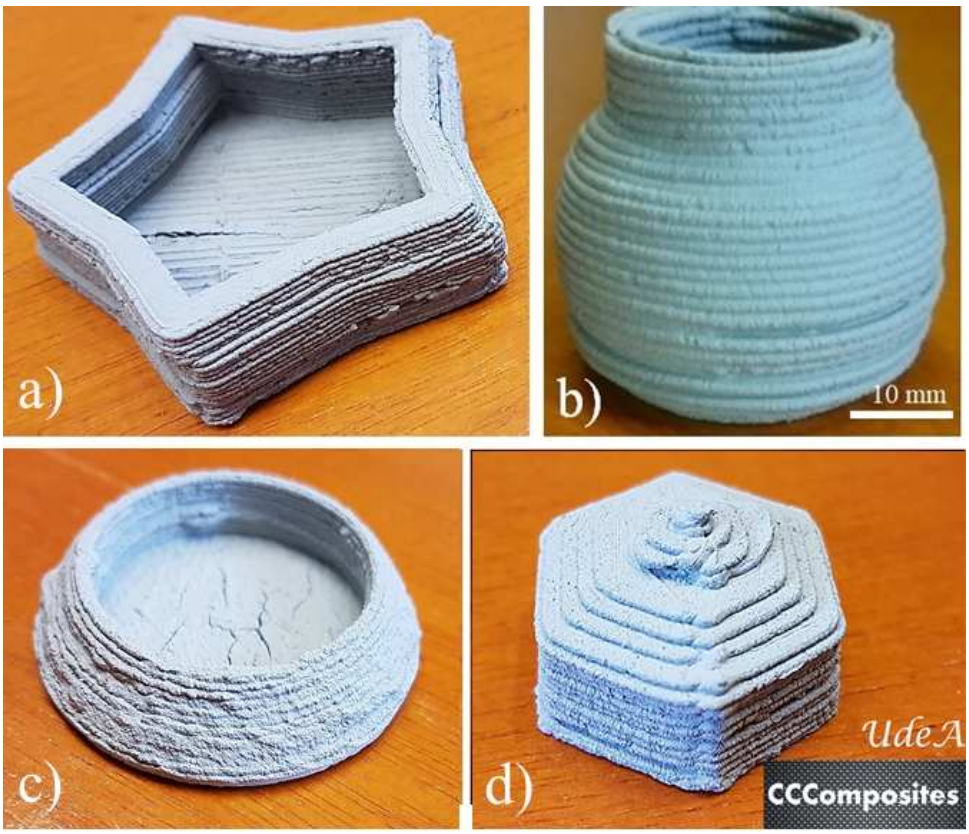

Figure 16. Samples fabricated by DIW using clay with fly ash addition: a) star bowl container, b) clay vase, c) trapezoidal bowl and d) hexagonal pyramid

The fly ash was found to be the best additive in this investigation for the kaolinite clay in terms of the surface finishing since different pieces were printed with this formulation.

IV. Discussion

The presented results support previous findings regarding the DIW technique and its high versatility for printing powdered ceramics and clays. Novel research has been reported with a similar material, kaolin [37], using water glass as an additive. However, no investigations were found reporting the use of the additives investigated here in combination with kaolinite clay. Moreover, even these very few researches found mostly focusses on processed kaolin as a high tech paste. Fly ash has been used in the 3D printing as a raw material for geopolymer concrete [38] with overall good results, but with limited surface finishing being worse than the presented in this paper. Certainly the chemical role of fly ash in the geopolymer is far more significant than in the clay material we are using, which is related to the geopolymer reaction. In the current research this material acts just as a property improver and filler of voids. One of the advantages of using fly ash and the other additives used in this investigation (talc and lime) is that 3D printing materials are still expensive for large scale applications [39] and not easily found in many countries. However, in this research fly ash enables the technique to be used by more people and have a greater impact to society.

In this investigation, overall, fly ash particles produced better results than other tested additives. This can be associated with several factors that include: the particle shape, particle distribution (Fig. 3 and 4) and also the chemical interaction of fly ash and clay. The first of all, results show that fly ash particles not only act as fillers but also have a significant contribution to the rheological behaviour, very important factor for the additive manufacturing. In terms of the particle shape, the spherical geometry works better for the flow of particles as they have the lowest restriction in terms of anchoring sides limiting the flow through the printing nozzle and so improving finishing of the parts. Because of this spherical particle shape, the mixture requires less water and encourages maximum particle packing to reduce porosity [40] and thus increase the compressive strength. Fly ash alone has insufficient plasticity to produce structures strong enough to survive handling and drying, it is the combination with clay that helps to successfully print and manufacture samples with complex shapes, in which samples showed a good degree of compaction under W/C of 0.70.

Fly ash has been widely used as pozzolanic material [41], which decreases the water absorption in the clay admixtures [42], improve the thermomechanical properties and cost of traditional bricks [36], and reduce waste absorption and processing temperature for tiles made

with clays and fly ash [43]. As mentioned before, beside this work, this material has been scarcely investigated before as additive for additive manufacturing.

Regarding the particle size distribution results, the particle size near 1 μm seems to be more influential for the overall investigated properties than other mean particle size curves. So, thanks to the incorporation of fly ash in the clay, the finer particles of fly ash fill the pores of the clay and contribute to the reduction of empty spaces and increase the strength of the mixture [44].

Moreover, the interactions of fly ash particles with water and clay showed to be more favourable for the DIW process used since the samples have better thermomechanical stability after the sintering process. These good results can be related to the high temperature formation of the fly ash as a by-product of the steel making industry [12, 45–47], and therefore associated to the good compressive strength results for samples after exposure to high temperatures.

This result was expected as the pozzolanic properties of fly ash in many systems including concrete are well-known. Thus the reactions of the combination clay-water-fly ash not only in the green body but also upon the exposure to high temperature contribute positively to the manufacturing process.

The mechanical strength variation in the samples with lime and talc can be explained by the presence of porosity caused mainly by the extrusion process. The complex shape promotes the presence of air (unless vacuum is used), because the presence of water in the samples favours the formation of pores and cracks when it evaporates, during the drying and sintering processes [48]. It is known that porosity in clay mixtures is associated with the clay sheets orientation along the extrusion plane [49] which certainly can occur in the printing process. This effect is hard to decrease as the clay particles orientation is not controllable by the DIW process used.

Surface finishing of the samples was clearly better in the clay-based samples containing fly ash. For this mixture the mechanical properties are not the best, but in comparison with the other additives, these properties are approximately constant in the different formulations. In addition, the effect of the calcium from fly ash particles has been investigated [50] showing poor performance when calcium content is low and the process is conducted under an acidic environment [51]. Other researches [52] have demonstrated an improvement in the mechanical properties by the addition of calcium-based compounds, such as CaO and $Ca(OH)_2$ [53]. Calcium compounds typically result in the precipitation of calcium silicate hydrates or calcium silicate aluminate hydrates phases, which improve the dissolution of the fly ash in the alkaline medium. Thus, the calcium content in fly ash can also positively influence the surface finishing of the samples.

On the other hand, some studies have shown that the mechanical properties of fired clay bricks are reduced by 39% for 10 wt.% addition of residues [54], which also supports why additives used in this research did not exceed 3 wt.%. The compressive strength is affected by the defects inside the sample, but also by those generated at the sample surface. Therefore, a lot of the improvement could be obtained if the process is conducted with an optimized ceramic paste, printed in an optimized process, thus obtaining a smoother surface finishing that does not adversely affect the mechanical response.

XRD showed a significant content of mullite, which confers interesting properties to clay ceramics such as chemical stability, mechanical resistance, low expansion at high temperatures, resistance to thermal shock, resistance to mechanical abrasion and erosion by flame, resistance to the attack of slag and molten metals and the corrosive action of glass [55]. In addition, under normal pressures and conditions of sintering and use, mullite is the only compound of alumina and silica stable at high temperatures [56]. Moreover, the necessary percentages of additives to guarantee the permanence of the pozzolanic reactions (durability, impermeability, resistance to cracking and strong and flexible structural layer) over time vary between 3 wt.% and 7 wt.% with respect to the weight of the clay [57]. Therefore, the content of additives used is justified in order to keep these pozzolanic reactions stable and because percentages higher than 10 wt.% are unsuitable because of the excessive drying shrinkage [54].

On the other hand, most clays are composed of about 65 wt.% silica and 20 wt.% alumina. They may also contain varying amounts of other metallic oxides like manganese, phosphorus, calcium, magnesium, sodium, potassium and vanadium oxides [58]. The addition of materials such as lime, fly ash and talc, can result in a deterioration of the surface finishing of the samples because of the presence of high content of silicates, alumina, free lime and some oxides. They allow a pozzolanic reaction with clays and can cause a reduction in the rate of expansion [59].

Regarding the kaolin particles, these are characterized by both a negative face and a positive face electrical charge [60]. This heterogeneous charge behaviour is responsible for the positive-negative charge attraction between particles, giving rise to a range of clay microstructures such as card-house and band-like structures [61]. This variable microstructure and complex charging behaviour can also be an important reason why the printed samples with kaolin, lime and talc show worse surface finishing when compared to samples with fly ash.

With the purpose of presenting more detailed information about the results showed in Fig. 6, an average between the results for contraction in diameter and height that came from the fly ash mixtures was estimated (Fig. 17). Diameter of the samples decreased as expected, but in general, height dimension was independent of W/C (Fig. 17a). This can only be explained as a consequence of the printing symmetry, which certainly confers prop-

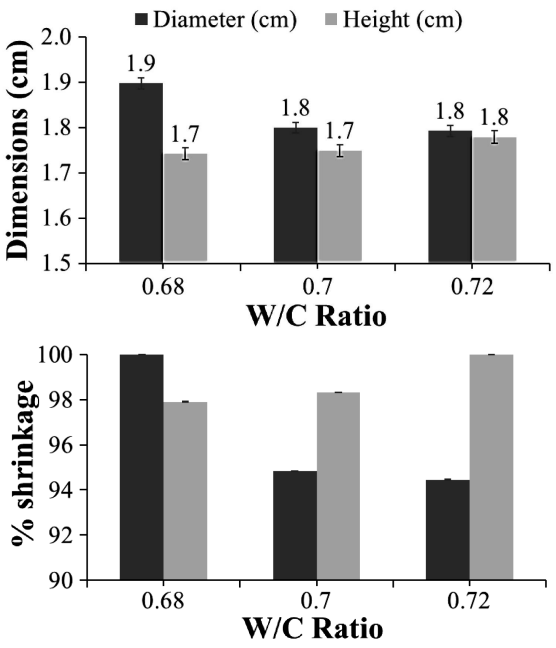

Figure 17. Stability tests average results for samples fabricated with clay and fly ash

erties depending of the direction. This can be confirmed by Fig. 17b where shrinkage over diameter and height has opposite trends depending on the W/C. From these results it can be concluded that for formulation W/C 0.7, the fly ash presents a more stable dimensional behaviour with respect to the diameter, as it is affected by temperature changes in the drying and sintering processes. In comparison with the other formulations the temperature causes a decrease in their dimensions (height and diameter).

In order to improve the printing process of these clay based materials using the DIW technique, the utilization of additives such as polyethylene glycol (PEG) and glycerine as flocculants could be a good option. If combined with fly ash particles these substances can reduce the pressure at the entrance of the nozzle thanks to its plasticizing properties in extrusion [62]. Likewise, it is suggested to use sodium polyacrylate as a deflocculant because this additive has favourable properties such as high effectiveness and easy dosing. The most valuable attribute of these deflocculation agents is primarily their beneficial effect on the properties of casting slip [63]. Besides the deflocculation effects of polyacrylates, they are connected with the distinctive property of adsorbing themselves on the surface of mineral particles [64].

A full study of the rheology and the optimization process of these clay mixtures, particularly the one with fly ash, is under a current evaluation for a large-scale process in the traditional ceramics industry, which certainly is the real proof. The rheology certainly is a crucial part of the process and therefore the research from lab has to be not only verified, but also modified for the new challenge. It is expected that this clay based material upon the beneficiation process, commonly done by the traditional ceramics manufacturing, and upon the use of surfactants, dispersants and flocculants to tailor the printing material will produce much better finishing of the printed parts.

It is widely reported [65] that clays are typically anisotropic materials. This originates from their layered structure which has been demonstrated not only for diverse clay types [66] but also by its effects on the properties [67]. Particularly, this effect in additive manufacturing and specifically in the DIW process can play an important role for the parameters such as the flow and sample printability, since elasticity and strain related properties can be significantly affected by the anisotropy [65]. In kaolinite clays the effect is also well-known [68] although it has not been investigated in additive manufacturing. Therefore, the understanding and further exploitation of clays anisotropy for DIW is open up for investigation and perhaps for a significant improvement of the technique.

Finally, it is important to mention that the current results enable DIW technique to be used elsewhere by anybody, which was partially the goal of this research. Therefore, the processing technique as well as the additives used are not only inexpensive but available worldwide. Although the finishing of the surfaces has some limitations, it is important to know that this sample quality is useful for many applications in the largest materials industry by volume and weight worldwide, the construction and building materials industry. Applications such as facades, urban furniture, and decoration can be available with this technique.

V. Conclusions

Direct ink writing technique (DIW), an extrusion based additive manufacturing process, has been used to fabricate kaolinite clay based-ceramics with several inexpensive ceramic additive powders: lime, fly ash and talc. The samples were fabricated with water to clay ratios (W/C) between 0.68 and 0.72. The additives were tested in 3.0, 5.0 and 7.0 wt.% with respect to the clay contents and it was confirmed that the samples with 3 wt.% additives showed the best performances. The obtained results also showed that samples with 0.70 W/C ratio and fly ash as an additive were the best in terms of workability, mechanical properties and surface finishing.

The process and materials presented in this research open up the possibility of traditional industries to really think in the implementation of additive manufacturing as a complement to traditional methods, which can also be seen as an innovation line of the company. Moreover, the process and materials are adaptable to individuals.

Acknowledgement: The authors wish to thank Sumicol S.A.S. for its partial support in this investigation.

References

1. F. Bergaya, G. Lagaly, "General introduction: clays, clay minerals, and clay science", *Dev. Clay Sci.*, **1** (2006) 1–18.

2. W.M. Bundy, J.N. Ishley, "Kaolin in paper filling and coating", *Appl. Clay Sci.*, **5** [5] (1991) 397–420.
3. R.E. Grim, *Applied Clay Mineralogy*, McGraw-Hill, New York, 1962.
4. L.T. Drzal, J.P. Rynd, T. Fort Jr., "Effects of calcination on the surface properties of kaolinite", *J. Colloid Interface Sci.*, **93** [1] (1983) 126–139.
5. A. Russel, "Minerals in pharmaceuticals, the key is quality assurance", *Ind. Miner.*, **251** (1988) 32–43.
6. P. Ptáček, F. Šoukal, T. Opravil, M. Nosková, J. Havlica, J. Brandštetr, "The kinetics of Al-Si spinel phase crystallization from calcined kaolin", *J. Solid State Chem.*, **183** [11] (2010) 2565–2569.
7. D.G. Williams, C.L. Garey, "Crystal imperfections with regard to direction in kaolinite mineral", *Clays Clay Miner.*, **22** (1974) 117–125.
8. C. García-Portillo, J. Bastida, P. Pardo, G. Rodríguez-López, M.J. Lacruz, M.L. Vilar, A. Lázaro, "Influencia de características microestructurales de caolinita en las propiedades de sus pastas de colaje", *Bol. Soc. Esp. Ceram. Vidr.*, **44** (2005) 239–244.
9. J. Konta, "Clay and man: clay raw materials in the service of man", *Appl. Clay Sci.*, **10** [4] (1995) 275–335.
10. H.A. Colorado, H.T. Hahn, C. Hiel, "Pultruded glass fiber- and pultruded carbon fiber-reinforced chemically bonded phosphate ceramics", *J. Compos. Mater.*, **45** [23] (2011) 2391–2399.
11. H.A. Colorado, C. Hiel, H.T. Hahn, "Chemically bonded phosphate ceramics composites reinforced with graphite nanoplatelets", *Compos. Part A Appl. Sci. Manuf.*, **42** [4] (2011) 376–384.
12. A. Loaiza, S. Cifuentes, H.A. Colorado, "Asphalt modified with superfine electric arc furnace steel dust (EAF dust) with high zinc oxide content", *Constr. Build. Mater.*, **145** (2017) 538–547.
13. C.F. Revelo, H.A. Colorado, "3D printing of kaolinite clay ceramics using the Direct Ink Writing (DIW) technique", *Ceram. Int.*, **44** (2018) 5673–56.
14. J.A. Lewis, J.E. Smay, J. Stuecker, J. Cesarano, "Direct ink writing of three-dimensional ceramic structures", *J. Am. Ceram. Soc.*, **89** [12] (2006) 3599–3609.
15. J.A. Lewis, "Direct ink writing of 3D functional materials", *Adv. Funct. Mater.*, **16** [17] (2006) 2193–2204.
16. I. Gibson, D.W. Rosen, B. Stucker, *Additive Manufacturing Technologies*, Vol. 238, Springer, 2010.
17. J.H. Song, M.J. Edirisinghe, J.R.G. Evans, "Formulation and multilayer jet printing of ceramic inks", *J. Am. Ceram. Soc.*, **82** [12] (1999) 3374–3380.
18. J.J. Beaman, C.R. Deckard, "Selective laser sintering with assisted powder handling", *Google Patents*, 03-Jul-1990.
19. E.B. Duoss, M. Twardowski, J.A. Lewis, "Sol-gel inks for direct-write assembly of functional oxides", *Adv. Mater.*, **19** [21] (2007) 3485–3489.
20. W. Bian, D. Li, Q. Lian, X. Li, W. Zhang, K. Wang, Z. Jin, "Fabrication of a bio-inspired beta-tricalcium phosphate/collagen scaffold based on ceramic stereolithography and gel casting for osteochondral tissue engineering", *Rapid Prototyp. J.*, **18** [1] (2012) 68–80.
21. J.D. Cawley, A.H. Heuer, W.S. Newman, B.B. Mathewson, "Computer-aided manufacturing of laminated engineering materials", *Am. Ceram. Soc. Bull.*, **75** [5] (1996) 77–82.
22. B.Y. Tay, J.R.G. Evans, M.J. Edirisinghe, "Solid freeform fabrication of ceramics", *Int. Mater. Rev.*, **48** [6] (2003) 341–370.
23. W. Li, A. Ghazanfari, D. McMillen, M.C. Leu, G.E. Hilmas, J. Watts, "Characterization of zirconia specimens fabricated by ceramic on-demand extrusion", *Ceram. Int.*, **44** (2018) 12245–12252.
24. D.B. Chrisey, "The power of direct writing", *Science*, **289** [5481] (2000) 879–881.
25. M. Dayioglu, B. Cetin, S. Nam, "Stabilization of expansive Belle Fourche shale clay with different chemical additives", *Appl. Clay Sci.*, **146** (2017) 56–69.
26. Y.-J. Yang, A.V. Kelkar, Xilan Zhu, G. Bai, H.T. Ng, D.S. Corti, E.I. Franses, "Effect of sodium dodecylsulfate monomers and micelles on the stability of aqueous dispersions of titanium dioxide pigment nanoparticles against agglomeration and sedimentation", *J. Colloid Interface Sci.*, **450** (2015) 434–445, 2015.
27. S. Mathur, "Kaolin flotation", *J. Colloid Interface Sci.*, **256** [1] (2002) 153–158.
28. S. Goldberg, H.S. Forster, "Flocculation of reference clays and arid-zone soil clays", *Soil Sci. Soc. Am. J.*, **54** [3] (1990) 714–718.
29. B.R. Phani Kumar, R.S. Sharma, "Effect of fly ash on engineering properties of expansive soils", *J. Geotech. Geoenvironm. Eng.*, **130** [7] (2004) 764–767.
30. P.F. Buitrago Restrepo, I. Duque Márquez, *The orange economy: An infinite opportunity*, Inter-American Development Bank, Washington, DC, 2013.
31. W.R. Stahel, "Circular economy", *Nature*, **531** [7595] (2016) 435–438.
32. E. Garzón, M. Cano, B.C. O'Kelly, P.J. Sánchez-Soto, "Effect of lime on stabilization of phyllite clays", *Appl. Clay Sci.*, **123** (2016) 329–334.
33. E.-J. Teh, Y.K. Leong, Y. Liu, A.B. Fourie, M. Fahey, "Differences in the rheology and surface chemistry of kaolin clay slurries: The source of the variations", *Chem. Eng. Sci.*, **64** [17] (2009) 3817–3825.
34. L. Pérez-Villarejo, D. Eliche-Quesada, F.J. Iglesias-Godino, C. Martínez-García, F.A. Corpas-Iglesias, "Recycling of ash from biomass incinerator in clay matrix to produce ceramic bricks", *J. Environ. Manage.*, **95** (2012) S349–S354.
35. R.J. Flatt, "Salt damage in porous materials: how high supersaturations are generated", *J. Cryst. Growth*, **242** [3] (2002) 435–454.
36. G. Cultrone, E. Sebastián, "Fly ash addition in clayey materials to improve the quality of solid bricks", *Constr. Build. Mater.*, **23** [2] (2009) 1178–1184.
37. Y. Zhou, A.M. LaChance, A.T. Smith, H. Cheng, Q. Liu, L. Sun, "Strategic design of clay-based multifunctional materials: From natural minerals to nanostructured membranes", *Adv. Funct. Mater.*, **29** (2019) 1807611.
38. B. Panda, M.J. Tan, "Experimental study on mix proportion and fresh properties of fly ash based geopolymer for 3D concrete printing", *Ceram. Int.*, **44** [9] (2018) 10258–10265.
39. N.M. Zain, N.H. Hassan, M. Ibrahim, M.S. Wahab, "Solid freeform fabrication of prototypes using palm oil fly ash via 3D printing", *J. Appl. Sci.*, **11** [9] (2011) 1648–1652.
40. P. Duxson, J.L. Provis, "Designing precursors for geopolymer cements", *J. Am. Ceram. Soc.*, **91** [12] (2008) 3864–3869.
41. P. Chindaprasirt, C. Jaturapitakkul, T. Sinsiri, "Effect of fly ash fineness on microstructure of blended cement paste",

Constr. Build. Mater., **21** [7] (2007) 1534–1541.
42. X. Lingling, G. Wei, W. Tao, Y. Nanru, "Study on fired bricks with replacing clay by fly ash in high volume ratio", *Constr. Build. Mater.*, **19** [3] (2005) 243–247.
43. A. Mishulovich, J. Evanko, "Ceramic tiles from high-carbon fly ash", paper 18 in *International ash utilization symposium*, Center for Applied Energy Research, University of Kentucky, 2003.
44. H.S. Mann, G.S. Brar, K.S. Mann, G.S. Mudahar, "Experimental investigation of clay fly ash bricks for gamma-ray shielding", *Nucl. Eng. Technol.*, **48** [5] (2016) 1230–1236.
45. C. Shi, "Steel slag - its production, processing, characteristics, and cementitious properties", *J. Mater. Civil. Eng.*, **16** [3] (2004) 230–236.
46. A. Loaiza, H.A. Colorado, "Marshall stability and flow tests for asphalt concrete containing electric arc furnace dust waste with high ZnO contents from the steel making process", *Constr. Build. Mater.*, **166** (2018) 769–778.
47. H.A. Colorado, E. Garcia, M.F. Buchely, "White ordinary portland cement blended with superfine steel dust with high zinc oxide contents", *Constr. Build. Mater.*, **112** (2016) 816–824.
48. W.D. Callister, *Materials Science and Engineering: An Introduction*, John Wiley Sons. Inc., New York, USA, 2007.
49. L.V. Korah, P.M. Nigay, T. Cutard, A. Nzihou, S. Thomas, "The impact of the particle shape of organic additives on the anisotropy of a clay ceramic and its thermal and mechanical properties", *Constr. Build. Mater.*, **125** (2016) 654–660.
50. P. Nath, P.K. Sarker, "Effect of GGBFS on setting, workability and early strength properties of fly ash geopolymer concrete cured in ambient condition", *Constr. Build. Mater.*, **66** (2014) 163–171.
51. S. Wallah, B.V. Rangan, "Low-calcium fly ash-based geopolymer concrete: Long-term properties", *Research Report*, Curtin University of Technology, Perth, Australia, 2006.
52. J. Temuujin, A. van Riessen, R. Williams, "Influence of calcium compounds on the mechanical properties of fly ash geopolymer pastes", *J. Hazard. Mater.*, **167** [1] (2009) 82–88.
53. J. Peyne, J. Gautron, J. Doudeau, E. Joussein, S. Rossignol, "Influence of calcium addition on calcined brick clay based geopolymers: A thermal and FTIR spectroscopy study", *Constr. Build. Mater.*, **152** (2017) 794–803.
54. I. Demir, "Effect of organic residues addition on the technological properties of clay bricks", *Waste Manage.*, **28** [3] (2008) 622–627.
55. H. Schneider, K. Okada, J.A. Pask, *Mullite and Mullite Ceramics*, John Wiley & Sons, Chichester, England, 1994.
56. L. Tcheichvili, M. Butschkowskyi, "Un aporte al problema de la mullita", *Bol. Soc. Esp. Cerám. Vidr.*, **14** [1] (1975) 9–22.
57. S. Hollanders, R. Adriaens, J. Skibsted, Ö. Cizer, J. Elsen, "Pozzolanic reactivity of pure calcined clays", *Appl. Clay Sci.*, **132-133** (2016) 552–560.
58. J. Eisenhauer Tanner, R.E. Klingner, "Clay Masonry Units" pp. 21–26 in *Masonry Structural Design*, Second Edition. McGraw Hill Education, USA, 2017.
59. J.F. Camacho Tauta, O.J. Reyes Ortiz, C. Mayorga Antolínez, D.F. Méndez, "Evaluation of additives used in the treatment of expansive clays", *Neogranadine Sci. Eng.*, **16** [2] (2006) 45–53.
60. P.-I. Au, Y.-K. Leong, "Surface chemistry and rheology of slurries of kaolinite and montmorillonite from different sources", *KONA Powder Part. J.*, **33** (2016) 17–32.
61. G. Lagaly, "Principles of flow of kaolin and bentonite dispersions", *Appl. Clay Sci.*, **4** [2] (1989) 105–123.
62. R. Nath Das, C.D. Madhusoodana, K. Okada, "Rheological studies on cordierite honeycomb extrusion", *J. Eur. Ceram. Soc.*, **22** [16] (2002) 2893–2900.
63. E. Alston, "Dispersing agents suitable for the deflocculation of casting slip", *Trans. Br. Ceram. Soc.*, **74** [8] (1975) 279–283.
64. G. Bigelow, S. Prokopovich, "Sodium polyacrylate – deflocculation mechanism in clay slips and some properties", *J. Aust. Ceram. Soc.*, **13** [2] (1977) 31–34.
65. C.M. Sayers, L.D. den Boer, "The elastic anisotropy of clay minerals", *Geophysics*, **81** [5] (2016) C193–C203.
66. S. Salager, B. François, M. Nuth, L. Laloui, "Constitutive analysis of the mechanical anisotropy of Opalinus Clay", *Acta Geotech.*, **8** [2] (2013) 137–154.
67. S. Fityus, O. Buzzi, "The place of expansive clays in the framework of unsaturated soil mechanics", *Appl. Clay Sci.*, **43** [2] (2009) 150–155.
68. J. Bourret, N. Tessier-Doyen, R. Guinebretiere, E. Joussein, D.S. Smith, "Anisotropy of thermal conductivity and elastic properties of extruded clay-based materials: Evolution with thermal treatment", *Appl. Clay Sci.*, **116-117** (2015) 150–157.